



Full paper/Mémoire

Surface reactivity of uranium hexafluoride (UF₆)Réactivité de surface de l'hexafluorure d'uranium UF₆

Bertrand Morel^{a, b}, Ania Selmi^{a, b}, Laurent Moch^{a, b},
 Jean-Michel Hiltbrunner^{a, b, c}, Mickael Achour^{a, b, c}, Rachid Benzouaa^{a, b, c},
 Aurélien Bock^{b, c}, Laurent Jouffret^{b, c}, Pierre Bonnet^{b, c}, André Hamwi^{b, c},
 Marc Dubois^{b, c, *}

^a Hall de recherche de Pierrelatte, Site AREVA du Tricastin, route du Site-de-Tricastin, 26701 Pierrelatte, France^b Laboratoire commun de recherche AREVA/CNRS/UCA, France^c Université Clermont Auvergne, CNRS, SIGMA Clermont, ICCF, 63000 Clermont-Ferrand, France

ARTICLE INFO

Article history:

Received 30 January 2018

Accepted 15 May 2018

Available online 23 June 2018

Keywords:

Uranium hexafluoride

Interface

Purification

Corrosion

Intercalation

Mots-clés:

Hexafluorure d'uranium

Interface

Purification

Corrosion

Intercalation

ABSTRACT

The present article reviews a selection of results obtained in the AREVA/CNRS/UCA joint research laboratory. It focuses on interfaces formed by uranium hexafluoride (UF₆) with chemical filter (purification), carbon (UF₆ storage), and metallic substrate (corrosion). As a matter of fact, along the nuclear fuel cycle, metallic surfaces of the fluorination reactors, cooling systems (for the liquefaction of UF₆), and storage containers are in contact with UF₆, either in the gas or in the liquid phase. For the removal of volatile impurities before the enrichment, surface of chemical filters with a high specific surface area must be enhanced for both selectivity and efficiency. To store depleted UF₆ (²³⁸U), graphite intercalation compounds are proposed and preliminary results are presented.

© 2018 Académie des sciences. Published by Elsevier Masson SAS. This is an open access article under the CC BY-NC-ND license (<http://creativecommons.org/licenses/by-nc-nd/4.0/>).

R É S U M É

Cet article présente une sélection de résultats obtenus au laboratoire commun de recherche AREVA/CNRS/UCA « Chimie du fluor ». Il se focalise sur les différentes interfaces formées par l'hexafluorure d'uranium UF₆ avec les filtres chimiques (purification), le graphite (stockage de UF₆) et les substrats métalliques (corrosion). En effet, au cours du cycle du combustible nucléaire, les surfaces métalliques des réacteurs de fluoration, les cristalliseurs (pour la liquéfaction de UF₆) et les conteneurs sont en contact avec UF₆ sous ses formes gazeuse et liquide. Pour la séparation des impuretés volatiles avant l'enrichissement de UF₆, la surface des filtres chimiques doit être optimisée pour atteindre la sélectivité et l'efficacité. Enfin, pour stocker UF₆, en particulier celui riche en ²³⁸U sous-produit de l'enrichissement, des composés d'intercalation du graphite sont proposés et des résultats préliminaires sont donnés.

© 2018 Académie des sciences. Published by Elsevier Masson SAS. This is an open access article under the CC BY-NC-ND license (<http://creativecommons.org/licenses/by-nc-nd/4.0/>).

* Corresponding author.

E-mail address: Marc.dubois@uca.fr (M. Dubois).

1. UF₆: a key compound for nuclear industry

Uranium hexafluoride (UF₆) plays a key role in the nuclear industry. Its annual worldwide production of around 60,000 tons in 2010 is devoted to this application [1,2]. Most of the 500 commercial nuclear power reactors in the world today require uranium enriched in the ²³⁵U isotope for their fuel; only ²³⁵U can release energy by fission. Both the commercial and under development isotopic enrichments involve a gaseous uranium compound. The commercial processes are diffusion and centrifugation, whereas laser excitation is under development. UF₆, the only volatile compound of uranium, sublimes at 56.2 °C despite its high molecular weight. This property is combined with the relative chemical stability of UF₆. Moreover, fluorine has only a single stable naturally occurring isotope (¹⁹F) and only two isotopomers of UF₆ exist and differ in their molecular weight only because of the presence of ²³⁵U and ²³⁸U [1–5].

1.1. Isotopic enrichments

Uranium is a chemical element present in almost all media (rocks, water, etc.) often in very small proportions (from several hundreds of grams to several kilograms of uranium per ton of extracted minerals). However, in some exceptional cases, uranium content may reach few tens of kilograms of extracted minerals. Whatever uranium content in the minerals is used for its extraction, U is present mainly in two isotopic forms, namely 0.71% of ²³⁵U (fissile) and 99.28% of ²³⁸U (fertile). Uranium with ²³⁵U content between 3% and 5% is required for fuel in nuclear power reactors. Therefore, a uranium enrichment process is necessary. UF₆ is a colorless gas above 64 °C and a white solid at room temperature. The liquid phase exists only under pressures greater than about 1.5 atm and at temperatures above 64 °C. The triple point of UF₆ at 64 °C is used whatever the enrichment processes, gas diffusion, centrifugation, or laser excitation. All these processes are described below.

The gaseous diffusion process is based on the small mass difference between the two uranium isotopes. UF₆ gas is forced to diffuse under pressure through micropores of ceramics with a radius lower than the main free path of the molecules. The lighter molecules (²³⁵UF₆) diffuse slightly faster than the ²³⁸UF₆ molecules. Therefore, the enriched fraction is injected to the upper level and the depleted fraction comes back to the lower level. This process is repeated in cascade more than 1000 times to reach UF₆ containing ²³⁵U between 3% and 5%.

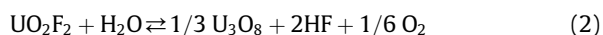
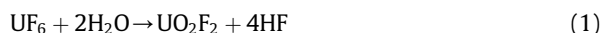
The gaseous diffusion requires much higher energy than the gas centrifuge process. Moreover, although the volume capacity of a single centrifuge is much smaller than that of a single diffusion stage, its efficiency to separate isotopes is higher. Centrifugation stages are also performed in cascade (centrifuges in parallel) but their number may only be 10–20. For these reasons, the use of diffusion process then decreased from 50% in 2000 to 25% in 2010 [1]. At the same time, centrifugation part increased to 40% in 2000, 65% in 2010, and 100% in 2015.

The centrifugation process also takes benefit from the mass difference between the two isotopes of gaseous UF₆.

The later is introduced into centrifuge rotating at a high speed (50,000–70,000 rpm). Thousands of cylinders are positioned in series. The lighter molecules with ²³⁵U are concentrated at the center of the centrifuge (the heavier ones with ²³⁸U increase in concentration toward the outer edge of the cylinder). A vertical separation is established with a gradient from the lighter at the top to the heaviest at the bottom. The countercurrent flow set up by a thermal gradient enables enriched product to be drawn off axially. The enriched fraction is collected from the head of the centrifuge and the depleted one at the bottom.

Laser enrichment processes are under investigation and the part of enriched U from this technique is expected to reach several percents in 2020. Photoionization may be performed either on uranium metal or on UF₆. In the atomic process, a powerful laser is used to ionize atoms in uranium metal vapor. The laser frequency is tuned to ionize ²³⁵U atoms but not ²³⁸U ones resulting in an electron ejection. The positively charged ²³⁵U ions are then attracted to a negatively charged plate and collected. The laser may act on U-containing molecule; its frequency tuning allows the breaking of one U–F bond involving ²³⁵U and not ²³⁸U. The photodissociation of ²³⁵UF₆ results in solid ²³⁵UF₅⁺, which can be easily separated from the unaffected gaseous UF₆ molecules containing ²³⁸U atoms.

The enriched UF₆ is then converted by chemical reduction to uranium oxide (UO₂) packaged as small pellets of 10 g. After sintering at high temperature, these pellets are then introduced in long hermetically closed metallic tubes (typically up to 4 m long) composed of zirconium alloys. Many fuel rods constitute a fuel assembly, which is ready to be loaded into the nuclear reactor. Depleted UF₆ (²³⁸U enriched UF₆), which is useless until now, is then stored as such or hydrolyzed into depleted uranium oxide U₃O₈ according to the following reactions:



Storage, as well as hydrolysis, is costly. Moreover, reactions may occur with containers. It is of primary importance to investigate the surface reaction of UF₆, both in the gas and liquid phases, with metallic containers. Whatever the technology used, any volatile impurities in UF₆ disturb the enrichment process as well as the corrosion in UF₆, the purification must be deeply investigated. With such aim, the physical–chemical properties of both UF₆ and the intermediate uranium fluorides must be considered. The intermediate fluorides are compounds of formula UF_x, where 4 < x ≤ 5. U₄F₁₇ (=UF_{4.25}), U₂F₉ (UF_{4.5}), and UF₅ have been reported as distinct compounds. This will be discussed in the following section.

1.2. UF₆ synthesis and physical–chemical properties

Various fluorinating agents may be used for the synthesis of UF₆: gaseous fluorine F₂, halogen fluorides, either liquid or gaseous (ClF₃, BrF₃, BrF₅, IF₇, etc.) [6], certain metal fluorides (CoF₃), and hydrogen fluoride [7,8]. Katz and Rabinowitch [9] and Tananaev et al. [7] review the

numerous routes. The panel of precursors using F_2 gas in the 200–400 °C range is also wide: metallic U, uranium carbide, U_3O_8 , UO_2 , UF_4 , intermediate fluorides, uranyl fluoride, double salts of the type KUF_5 and K_2UF_6 , and sodium diuranate. Fig. 1 summarizes the various routes to prepare UF_6 using F_2 . Both liquid and gaseous halogen fluorides (ClF_3 , BrF_3 , BrF_5 , and IF_7) are efficient to prepare UF_6 starting with metallic uranium [6].

Anhydrous hydrofluoric acid must be combined with an additional step with F_2 to increase uranium oxidation state to +VI as in the industrial process (see below). Nevertheless, a route starting with uranium pentachloride, UCl_5 , is reported [6]. It involves the double disproportionation of UF_5 formed from UCl_5 with HF. UF_5 forms UF_6 and U_2F_9 ; the latter disproportionates into UF_6 and UF_4 (heating allows the separation of solid UF_4 and UF_6).

The industrial process to obtain UF_6 from the ores takes place according to the following steps: (1) conversion of U_3O_8 into $UO_2(NO_3)_2$ using HNO_3 , (2) synthesis of UO_3 , and (3) reduction into UO_2 . In the two last steps, UO_2 with hydrofluoric acid (HF) is converted to UF_4 and then the oxidation with fluorine gas finally yields UF_6 .



The very exothermic conversion of UF_4 to UF_6 is performed in a flame reactor where temperature of about 1100 °C can be reached.

Uranium is only weakly radioactive and the chemical toxicity of UF_6 is more significant than its radiological toxicity. UF_6 is an oxidant and a mild Lewis acid [10–13]. It reacts with many elements such as Al, Ga, C, and so forth to form their fluorides and attacks many metals except Ni and Al on which a passivating and protective metal

fluoride layer is formed. In other words, UF_6 is a strong fluorinating agent. It does not react with oxygen, nitrogen, carbon dioxide, and halogens (in vapor phase). However, it is very hygroscopic and reacts with water to give uranyl fluoride (UO_2F_2) and HF. Uranium hexafluoride forms a very corrosive material (HF, hydrofluoric acid) when exposed to moisture.

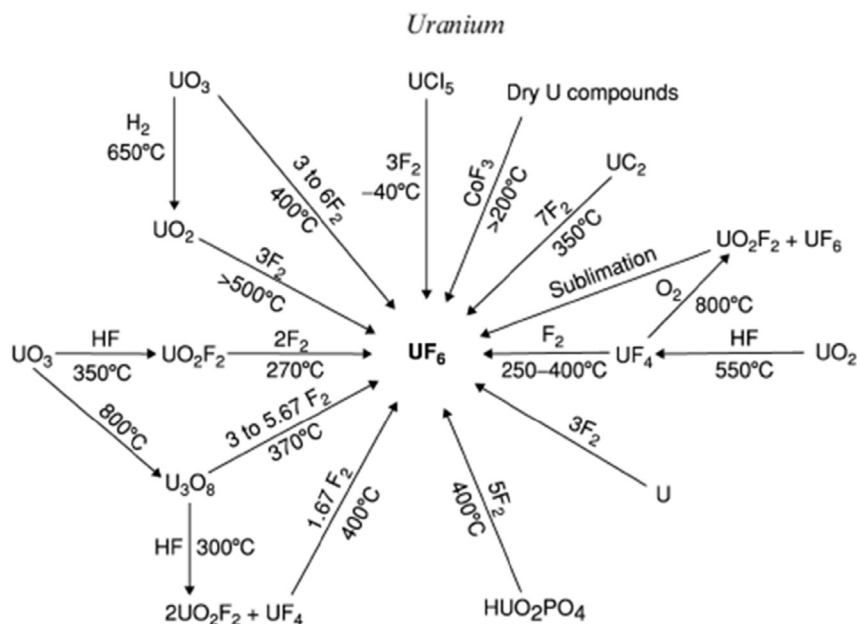
UF_6 being a strong fluorinating agent, its reaction with metallic uranium results in intermediate uranium fluorides according to the reaction



The resulting compounds depend on both the temperature and the pressure of UF_6 . Nevertheless, the products are unstable in absence of UF_6 whatever the composition, that is, x in UF_x . UF_4 and UF_6 are then formed. Reaction of either F_2 or UF_6 with solid UF_4 results also in intermediate uranium fluorides [7,14,15]. The reaction



takes place at a temperature lower than 250–260 °C at which hexafluoride is formed. The formation of intermediate fluorides may also occur during the fluorination of UF_4 with F_2 at higher temperature at which UF_6 is expected. This diffusion effect is due to the concentration of fluorine, which is lower in the bulk of the tetrafluoride layer than at the surface. The common feature of all intermediate uranium fluorides U_4F_{17} , U_2F_9 and UF_5 (α - and β -forms) is their ability to disproportionate. Agron's diagram indicates the stability of each compound as a function of UF_6 pressure (from a few millibars to around 15 bar) and temperature [14,15]. The studied UF_6 pressure range was in between a few millibars to around 15 bar. U_2F_9 , UF_5 , and U_4F_{17} were evidenced during this study. These intermediate fluorides exhibit common hydrolytic



disproportionation, the reaction with moisture giving UF₄, UO₂F₂, and HF whatever the fluorides, for instance:



1.3. AREVA/CNRS/UCA joint research laboratory

Along the nuclear fuel cycle, different surfaces are in contact with UF₆, either in the gas or in the liquid phase. Among them, metallic surfaces of the fluorination reactors, cooling systems (for the liquefaction of UF₆), and storage containers may react with UF₆ in particular when HF is present. Moreover, to increase the efficiency of the process the removal of volatile impurities is important before the enrichment step. Chemical filters with a high specific surface area (SSA) may be used for such aim resulting in UF₆/filter reactive interface. Finally, the diffusion effect of the fluorinating agent of UF₄ during the preparation of UF₆ involves also different interphases F₂/UF₄, UF₆/UF₄, UF₆/intermediate fluoride, and so forth. These interfaces, and the reactivity of UF₆ with the surface of different substrates are investigated in the AREVA/CNRS/UCA joint research laboratory since 2004 (located both at the Institute of Chemistry of Clermont-Ferrand and in the Research hall in Pierrelatte). The work started with the updating of Agron's diagram in the low pressure range and resulted in a better understanding of the formation of intermediate uranium fluorides. Purification of UF₆ using a chemical filter is the second main topic with the establishment of sorption abilities and mechanisms of both volatile impurities and UF₆ onto the filter surface. More recently, corrosion mechanisms and kinetics of metallic substrates in the presence of either liquid or gaseous UF₆ are under investigation. The present article reviews a selection of results obtained in the laboratory. Interfaces formed by UF₆ with chemical filter (purification), carbon (UF₆ storage), and metallic substrate (corrosion) will be discussed next.

2. Chemical filter/UF₆ interface

Uranium hexafluoride is a key compound of the front-end nuclear fuel cycle. To provide nuclear fuel purity for companies, international standards were established and the allowed quantity of pollutants in nuclear pellets is limited [16]. Pollutants originate from both uranium ore, chemical products used during conversion process, and/or fission products of used uranium. All elements are fluorinated during UF₆ synthesis and depending on the element, the volatility and its solubility vary in UF₆ [17]. Several techniques allow UF₆ purification such as distillation in liquid or gaseous phase [18], gaseous diffusion [19], or chemical reaction involving a redox mechanism [20]. The AREVA Comurhex plant actually performs a chemical purification using tributyl phosphate and nitric acid as purifier agents. The treatment of nitric products is expensive and noxious for the environment. To have a greener process and reduce the industrial maintenance operations, purification with a chemical filter was developed in AREVA R&D facilities.

Magnesium fluoride is well known for its industrial applications as a catalyst [21] or for its optical properties [22]. But MgF₂ is also a chemical filter for removal of

technetium [23], molybdenum [24], or neptunium fluoride [25] from UF₆. For this study, the selected volatile impurity is vanadium oxyfluoride (VOF₃). To improve the efficiency of a catalytic agent, high SSA MgF₂ is synthesized by a sol–gel process [26,27]. This chemical reaction implies that hydroxyl groups remain in the final product. For VOF₃ sorption, pellets furnished by Nippon Puretec (Japan) or postfluorinated by molecular fluorine in the Institute of Chemistry of Clermont-Ferrand are chosen. Sorption performances are tested after exposure at 80 °C during 24 h in a sealed PTFE reactor. Characterization techniques (X-ray diffraction [XRD], solid-state NMR with fluorine, proton and vanadium nuclei, infrared, and Raman spectroscopies) are performed to provide the mechanism involved. Then, the removal of vanadium in a UF₆/VOF₃ gaseous mixture is performed.

To tailor the physical–chemical properties of a chemical filter, in particular the hydroxyl groups' content and SSA, a fluorination post-treatment was carried out on MgF₂. The higher the fluorination temperature, the lower the SSA (Fig. 2) and the lower the OH/F ratio in accordance with the literature [26,27]. This ratio was obtained from a fit of ¹⁹F-MAS NMR spectra (see a representative fit in Fig. 3). The increase in fluorination temperature increases the size of pores due to a coalescence phenomenon. Considering the fluorine NMR spectra, a shoulder relative to the interaction between hydroxyl groups and fluorine is present in commercial MgF₂ with higher intensity than in the post-fluorinated product. From fit of the NMR data (Fig. 3), the chemical formula of the chemical filter is estimated as MgF_{1.6}(OH)_{0.4} and MgF_{1.86}(OH)_{0.14} for the raw and post-fluorinated samples, respectively. After 24 h of sorption, the amount of vanadium trapped is higher in commercial MgF₂ than in the postfluorinated sample. XRD, Raman, and infrared spectroscopies as well as (¹⁹F/⁵¹V) NMR characterizations point out that hydroxyl groups are consumed while new MgF_{2-x}(VO₂F₂)_x vanadium oxyfluoride species are identified. Then, the suggested mechanism implies a chemisorption process in two steps: an oxygen–fluorine transfer reaction between MgF_{2-x}(OH)_x and VOF₃ and a substitution of OH groups in MgF₂ by vanadium oxyfluoride. Finally, a partial physisorption mechanism occurs

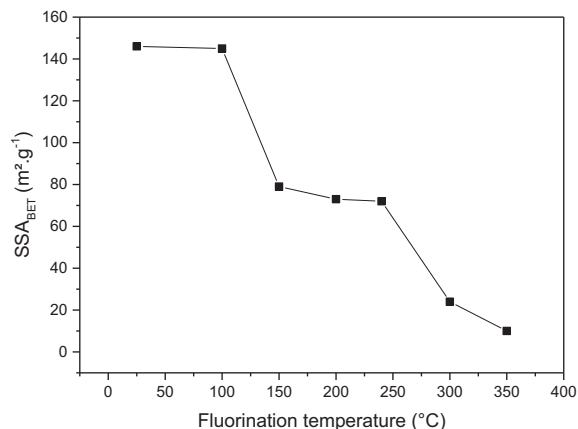


Fig. 2. Evolution of an SSA of MgF₂ as a function of fluorination temperature.

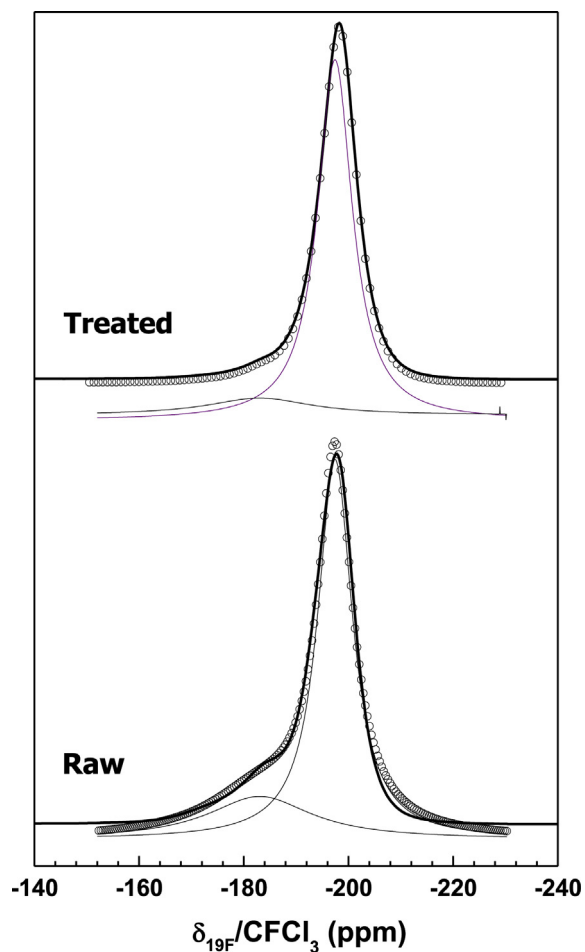


Fig. 3. Representative ^{19}F -MAS spectra of commercial and postfluorinated $\text{MgF}_{2-x}(\text{OH})_x$ (34 KHz).

at the surface of MgF_2 pellets, but the amount of vanadium trapped is smaller than in the chemisorption process.

Several attempts of VOF_3 removal in gaseous UF_6 were performed at the conversion R&D facility in Pierrelatte. Depending on the fluorination temperature of MgF_2 , the amount of uranium and vanadium adsorbed is modified (Fig. 4). For a fluorination at 100 or 200 °C, the amount of uranium trapped is higher than the vanadium due to a high OH/F ratio and the affinity of UF_6 to hydroxyl groups. For a fluorination at 250 and 300 °C, the quantity of reacting uranium drops whereas VOF_3 is better adsorbed. This fluorination treatment allows the selectivity of vanadium regarding UF_6 reaction. Above 300 °C, the amounts of pollutant and uranium reacting are reduced because of the diminution of OH groups present in MgF_2 . The understanding of the mechanism of sorption of volatile species onto MgF_2 and their selectivity in comparison with uranium hexafluoride allow the establishment of an operating mode to recycle the chemical filter MgF_2 for further sorptions. The recycling process involves a multistep treatment with NaOH as a key reactant to remove vanadium species and to regenerate OH groups.

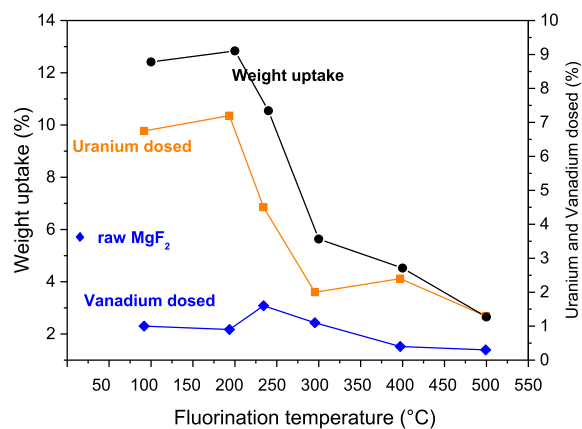


Fig. 4. Evolution of the amount of uranium and vanadium trapped as a function of MgF_2 fluorination temperature.

3. Carbon/ UF_6 interface

Except in France where it is converted into U_3O_8 , depleted UF_6 (with ^{238}U) is stored as such. A storage strategy may consist in the intercalation into a host matrix. UF_6 , as many other metallic fluorides [28–30], may be intercalated into graphite. Such a process is thermodynamically favorable [31,32]. KS15 graphite was used as a host matrix to prove the concept.

To reach the lowest graphite intercalation compound (GIC) stage, that is the highest content of U, the UF_6/C ratio was adjusted. KS15 graphite was placed in a passivated nickel boat in the reactor. The operating conditions are summarized in Table 1, including duration, temperature, molar quantity, and weight as well as weight and molar uptakes after reaction. The powder was outgassed under primary vacuum for 30 min in a reactor starting at room temperature and during the heating up to the reaction temperature. UF_6 was then injected in the reactor. The quantity of UF_6 remained constant through a continuous UF_6 flux (dynamic mode) except for the manipulation at 140 °C. After a few days of reaction (2–5 days), the reactor was cooled while the UF_6 in excess was removed by condensation into a trap cooled at 77 K. The expected GIC was then weighed.

The volume expansion and weight uptake evidence the formation of the GIC; the sample color changed from black to blue. As seen in Table 1, the final weight is approximately 10 times higher than the initial one (the molecular weight of UF_6 explains these huge uptakes). The weight and molar uptakes allow the C/U ratio to be calculated. XRD analysis underlines the formation of the $\beta\text{-UF}_5$ phase (Fig. 5).

The intercalation of metal fluorides into graphite takes place through a redox process. Carbon acts as an electron acceptor whereas the fluoride as a donor. The reactive unit consists of 24 carbon atoms. In most of the cases, the intercalation occurs through a direct contact of the fluoride with the host matrix. Nevertheless, the process may be catalyzed by the presence of F_2 , HF, or Cl_2 [28]. Taking into account that the intercalation of UF_6 into graphite occurs similarly as for WF_6 and MoF_6 , which exhibit similarities for

Table 1
Operating conditions for intercalation of UF₆ into graphite.

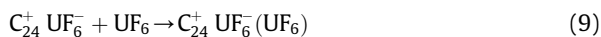
Temperature (duration)	80 °C (5 days)		100 °C (3 days)		120 °C (3 days)		140 °C (2 days)	
Graphite	Weight (g)	Quantity (mmol)	Weight (g)	Quantity (mmol)	Weight (g)	Quantity (mmol)	Weight (g)	Quantity (mmol)
	0.105	8.75	0.5046	42.05	0.2827	23.56	0.1566	13.05
UF ₆	Pressure (mbar)	Quantity (mmol)	Pressure (mbar)	Quantity (mmol)	Pressure (mbar)	Quantity (mmol)	Pressure (mbar)	Quantity (mmol)
	Dynamic ^a		Dynamic ^a		Dynamic ^a		1240	3.17
Uptake	Weight (g)	Quantity (mmol)	Weight (g)	Quantity (mmol)	Weight (g)	Quantity (mmol)	Weight (g)	Quantity (mmol)
	1.0255	2.91	6.3734	18.11	2.7156	7.71	1.1076	3.15
C/U	3		2.32		3.05		4.15	

^a Continuous flux of UF₆ (10 mL/min).

chemical and crystallographic properties [28], the redox process is

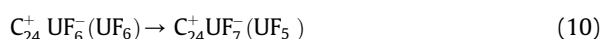


When the process goes further, additional neutral UF₆ molecules may be intercalated.

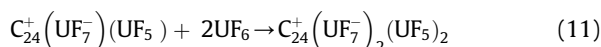


Nevertheless, XRD diagram indicates the presence of β -UF₅ phase. The hypothesis suggests that two UF₆ reactions

may be performed. In accordance with the tendency for disproportionation of uranium fluoride, such process forms UF₅ and UF₇:



The intercalation may go further to bring two more UF₆.



C₆UF₆ formula results from this mechanism, that is, a C/U ratio of 6. It is two times lower than the measured one. A higher intercalation rate seems to be formed because the intercalation was performed at temperatures between 80 and 140 °C, instead of room temperature, intercalation being a thermally activated process. Because the pattern of UF₅ dominates the XRD diagram, the GIC signature is masked for this sample. UF₆ being a strong fluorinating agent, the fluorination of the carbonaceous surface may also occur as



To validate these hypotheses, the addition of UF₆ has been controlled (at 140 °C, see Table 1). The resulting C/U ratio was 4.15 in accordance with the lower amount of UF₆. The formation of UF₅ is also limited, and XRD diagram of the resulting sample (Fig. 5b) exhibits the reflection for both the β -UF₅ and UF₆-GIC of first stage mainly (Table 2).

It is interesting to note that the identity period of 8.87 Å is slightly greater than the value given by Hagiwara et al. [32] (8.5 Å). This difference may be explained by the nature of the intercalated species. Hagiwara et al. assumed an insertion mechanism for which only UF₆ enters into the graphitic structure, as well as for its thermodynamic calculations. The insertion mechanism proposed here assumes the formation of UF₇ in the graphite host. The slightly larger size of UF₇ when compared with UF₆ may

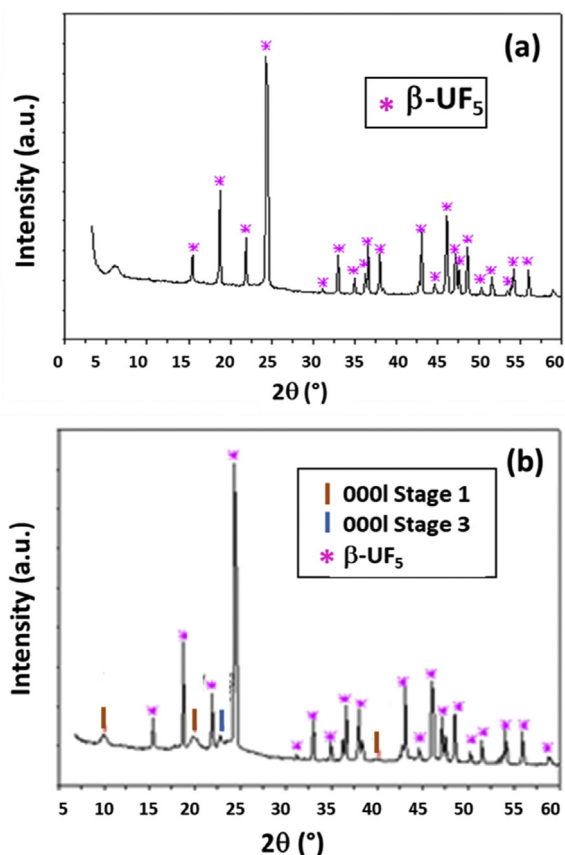


Fig. 5. XRD diagram of UF₆-GIC prepared (a) at 100 °C for 3 days (C/U = 2.32) and (b) at 140 °C for 2 days (C/U = 4.15).

Table 2
XRD data for UF₆-GIC (140 °C for 2 days).

Reflection	d (Å)	Stage
0001	8.87	1
0002	4.44	1
0004	3.88	3
0004	2.24	1

explain the difference in the identity period. The intercalation of UF_6 into graphite allows the low-temperature β - UF_5 phase to stabilize. Agron's diagram indicates that this phase is stabilized only for temperatures lower than 120°C . In our case, an intercalation at 140°C results in the same phase. Moreover, the stabilization of (α or β)- UF_5 phase is not possible without equilibrium with gaseous UF_6 . In the absence of UF_6 , UF_5 decomposes into UF_4 and UF_6 as for all of the intermediate uranium fluorides (see Section 1.3). In other words, (α or β)- UF_5 is stabilized by the graphitic matrix in our study. This opens new routes for both the storage of UF_6 and the stabilization of intermediate uranium fluorides.

4. Metal/ UF_6 interface

The industrial synthesis of UF_6 is the hydrofluorination of uranium mining concentrates through a process called conversion. The first stage aims at obtaining UF_4 from the mining concentrate, then converting this UF_4 to UF_6 , and finally storing UF_6 before its use in the enrichment process. During these stages, the uranium compounds will interact with different metal linings of the fluorination ovens, the piping in the industrial site, and the walls of the containers. Several kinds of metal interactions have thus to be taken into account: the cupronickel Monel of fluorination ovens and the different steel grades of the piping. Given the wide range of temperatures at which the uranium compounds are treated, the structural materials of Comurhex, the industrial conversion plant of AREVA, are submitted to liquid, solid, and gaseous uranium hexafluoride. Although it has been shown that UF_6 is highly reactive with ceramics or organic compounds, the different industrial steel grades and cupronickel alloys adapted for industrial appliances due to their cost and mechanical properties are still going to be eventually corroded. Trace amounts of corrosion products can be found in the liquid UF_6 and this unwanted pollution can imply a significant deviation from the American Society for Testing and Materials (ASTM) norm and generate a rejection in the final product.

The studies led at joint research laboratory intend to provide some data on the corrosion of metallic alloys in liquid and gaseous UF_6 . Three types of materials were chosen: nickel and the cupronickel alloys such as Monel, industrial grade steels, and finally pure iron (99.9%). Nickel-rich samples and industrial alloys were studied at first to understand their behavior under different fluorination temperatures, before their test of exposition to gaseous UF_6 . To contain experiments with liquid UF_6 , a dedicated experimental setup called CORFU (CORrosion in uranium hexaFLUoride) was designed and built. The constraints of liquid UF_6 such as radiological environment, relatively high pressure, and high reactivity with moisture have been thoroughly taken into account with specific devices developed to perform reliable experiments. The corrosion experiments are performed over various time durations, from a few hours to several months. Corroded samples were observed and analyzed by XRD and prepared for further analysis by scanning electron microscopy (SEM) coupled with energy-dispersive spectroscopy (EDS).

The first studies focused on the cupronickel alloys, particularly Monel; they aimed at understanding the corrosion of furnaces during the hydrofluorination of treated uranium mining concentrates. Studies were led on standardized nickel or Monel samples with an emphasis on the role of passivation. Results proved a much higher resistance to gaseous fluorine attack after high temperature passivation. UF_6 corrosion was then undertaken on passivated samples. Results show the formation of uranium fluoride crystals, identified as mostly UF_4 . The crystals grow on top of a NiF_2 layer, which is compact for passivated samples, but fragile and porous otherwise (Fig. 6). The NiF_2

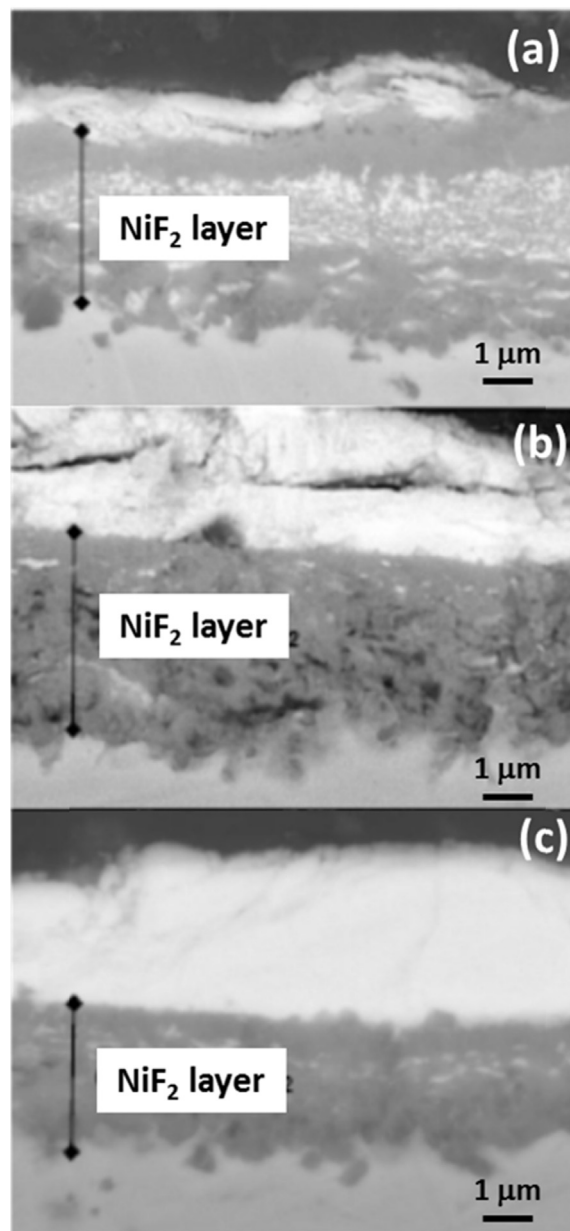


Fig. 6. SEM pictures of cross-sections of Monel exposed to UF_6 : (a) without pretreatment with F_2 , and pretreated in F_2 gas at (b) 200°C and (c) 450°C .

layer sits atop a copper rich surface of the samples. A proposed mechanism for Monel corrosion was developed. With unpassivated cupronickel alloys, UF_6 will react with Ni and Cu at the surface to form the corresponding fluoride species. Although the possibility of the formation of the $(\text{NiF}_2)_x(\text{UF}_6)_y$ can be proposed, it is probable that a nickel or uranium fluoride species play a role in the formation of a brittle NiF_2 layer. Copper, on the other hand, would form a highly volatile complex, unstable in UF_6 medium, which is easily transported. Gaseous UF_6 can diffuse through the porous nickel fluoride layer to continuously corrode the sample. In the case of a passivated sample, however, a compact NiF_2 acts as a protection barrier to UF_6 and slows considerably any diffusion of the gaseous species to initiate corrosion on the core material.

Although a mechanism was proposed for cupronickel alloys, the study of industrial steel alloys proved to be subject to a too high number of variables in play. The presence of Mo, W, or Si will cause volatile fluorides to be formed and leave cracked or fragile layers upon which uranium-rich crystals seed. The focus was put on the study of pure iron not only in gaseous but also in liquid UF_6 environments corresponding to the state at production

temperature. These results were obtained in the dedicated and reliable experimental CORFU setup, combined with procedures that were developed for this purpose. With SEM/EDS and XRD analyses, the corrosion nature was shown to be a layered structure, with an outer uranium fluoride layer on top of iron fluoride nodules or layers (Fig. 7), depending on the corrosion time. From XRD and EDS data, FeF_2 was found to be the iron fluoride formed in experimental conditions. It was formed initially as nodules before finally forming a layer subjected to cracks. The uranium fluoride compound's nature was not clearly identified by EDS because it is highly porous; only XRD results tend to show that a continuum of phases from U_2F_9 to UF_5 can be formed. Moreover, it has been shown that the uranium fluoride layer does not protect the metal and that the growth of the corrosion layer is because of the dissociation of UF_6 at a solid–solid interface and the diffusion of fluorine through the whole layer.

5. Conclusion

From the studies in the joint research laboratory, the conditions for formation of uranium fluorides, both single and

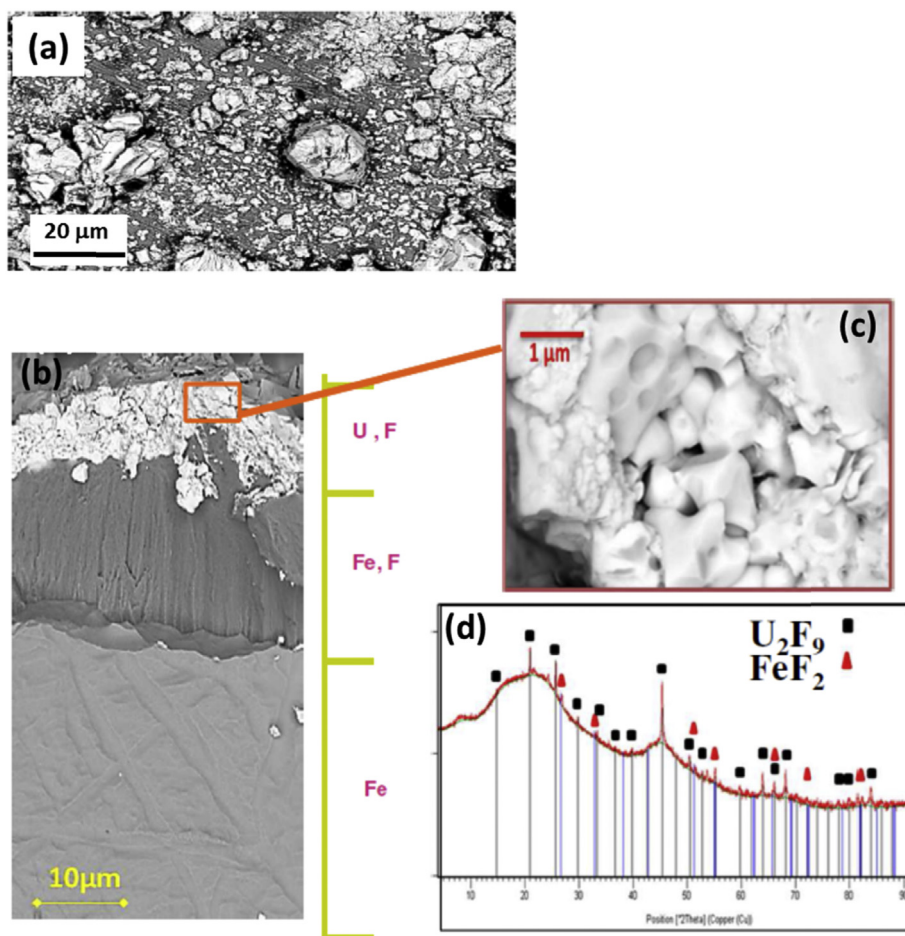


Fig. 7. SEM pictures of the continuous layer on an iron sample oxidized in liquid UF_6 : (a) general view of the corrosion layer, (b) cross-section, (c) zoomed uranium fluoride layer, and (d) XRD pattern.

intermediate, and their chemical properties are better understood. This allows different topics to be (re)investigated: corrosion involving either liquid or gaseous UF₆, removal of volatile impurities from UF₆, and storage of depleted UF₆. All these aspects are of both academic and industrial interests. The examples developed in the present article are representative of the joint research laboratory activities.

References

- [1] <http://www.world-nuclear.org>.
- [2] <http://www.avevgroup.com>.
- [3] P.D. Wilson (Ed.), *The Nuclear Fuel Cycle – From Ore to Wastes*, Oxford University Press, Oxford, UK, 1996.
- [4] P. Blanpain, G. Capus, J.-C. Palussière, *Chim. Int. J. Chem.* 59 (2005) 894–897.
- [5] B. Morel, B. Duperret, *J. Fluorine Chem.* 130 (1) (2009) 7–10.
- [6] O. Ruff, A. Heinzelman, *Z. Anorg. Chem.* 72 (1911) 63.
- [7] I.V. Tananaev, N.S. Nikolaev, Y.A. Luk'yanychev, A.A. Opalovskii, *Russ. Chem. Rev.* 30 (1961) 654.
- [8] L.E. Treverrov, J. Fischer, R.K. Stennenberg, *J. Am. Chem. Soc.* 79 (1957) 5167.
- [9] J. J. Katz, E. Rabinowitch, *The Chemistry of Uranium, Topics Manhattan Project, Uranium Compounds, Uranyl, Hexafluoride, Collection Folkscanomy Science; Folkscanomy; Additional Collections*.
- [10] J. Burdon, *Fluorinating Agents Introduction of Fluorine with High-valency Oxidizing Metal Fluorides*, 4th ed., Georg Thieme Verlag, Stuttgart, Germany, 1998.
- [11] P.J. Vergamini, *J. Chem. Soc. Chem. Commun.* (1979) 54–55.
- [12] A. Goosen, C.W. McClelland, P.J. Venter, M.W. Venter, *S. Afr. J. Chem.* 40 (1987) 30–34.
- [13] G.A. Olah, *Friedel–Crafts and Related Reactions*, Interscience, New York, 1963.
- [14] P.A. Agron, S.W. Weller, *Chem. Abstr.* 44 (1950) 7164.
- [15] J.M. Leitnaker, *Materials and Chemistry Technology Process Support*, 1983. Prepared for the U.S. Department of Energy Under U.S. Government Contract W-7405 eng 26.
- [16] ASTM, *Standard Specification for Uranium Hexafluoride for Enrichment*. ASTM Standard C787, 2015, p. 15.
- [17] N.S. Nikolaev, A.T. Sadikova, *Sov. Atom. Energy* 39 (5) (1975) 982–987.
- [18] A. Khan, A.R. Farooqui, M.A. Atta, *J. Chem. Soc. Pakistan* 22 (1) (2000) 9–13.
- [19] V.K. Ezhov, *Atom. Energy* 110 (3) (2011) 207–211.
- [20] P. Bergez, A. Deguelte, L. Seigneurin, *Process for the preparation of porous products based on cobalt fluoride or lead fluoride*. Brevet EP 0088006 A1, Commissariat à l'énergie atomique, France, 1983.
- [21] M. Wojciechova, M. Zielinski, M. Pietrowski, *J. Fluorine Chem.* 120 (2003) 1–13.
- [22] H. Schreiber, J. Wang, S. J. Wilkinso, *Durable MgO–MgF₂ Composite Film for Infrared Anti-reflection Coatings*, European Patent EP2715412, Corning Inc., 2012.
- [23] W. R. Gollhofer, *US Patent* 3165376, 1962.
- [24] D. Watanabe, A. Sasakira, K. Hoshino, F. Kawamura, *J. Nucl. Sci. Technol.* 48 (12) (2011) 1413–1419.
- [25] J. Ulhir, M. Marecek, *J. Fluorine Chem.* 130 (1) (2009) 89–93.
- [26] A. Demourgues, N. Penin, D. Dambournet, R. Clarenc, A. Tressaud, E. Durand, *J. Fluorine Chem.* 134 (2012) 35–43.
- [27] S. Wuttke, G. Scholtz, S. Rudiger, E. Kemnitz, *J. Mater. Chem.* 17 (2007) 4980–4988.
- [28] A. Hamwi, P. Touzain, L. Bonnetain, *Mater. Sci. Eng.* 31 (1977) 95–98.
- [29] A. Hamwi, S. Mouras, J.-C. Cousseins, *Synth. Met.* 34 (1-3) (1989) 97–102.
- [30] A. Hamwi, D. Claves, A. Senhaji, *J. Fluorine Chem.* 110 (2) (2001) 153–156.
- [31] J.L. Beauchamp, *J. Chem. Phys.* 64 (1976) 929.
- [32] R. Hagiwara, T. Fukui, H. Nakamura, Y. Ito, *J. Fluorine Chem.* 75 (1995) 209–213.